

AD-A152129

RIA-85-U45

AD A152129

AD-E401 303

TECHNICAL REPORT ARLCD-TR-84030

## METAL ARMATURES FOR RAILGUNS

GERALD L. FERRENTINO  
WILLEM J. KOLKERT

TECHNICAL  
LIBRARY

MARCH 1985



**U.S. ARMY ARMAMENT RESEARCH AND DEVELOPMENT CENTER**

**LARGE CALIBER WEAPON SYSTEMS LABORATORY**

**DOVER, NEW JERSEY**

**APPROVED FOR PUBLIC RELEASE; DISTRIBUTION UNLIMITED.**

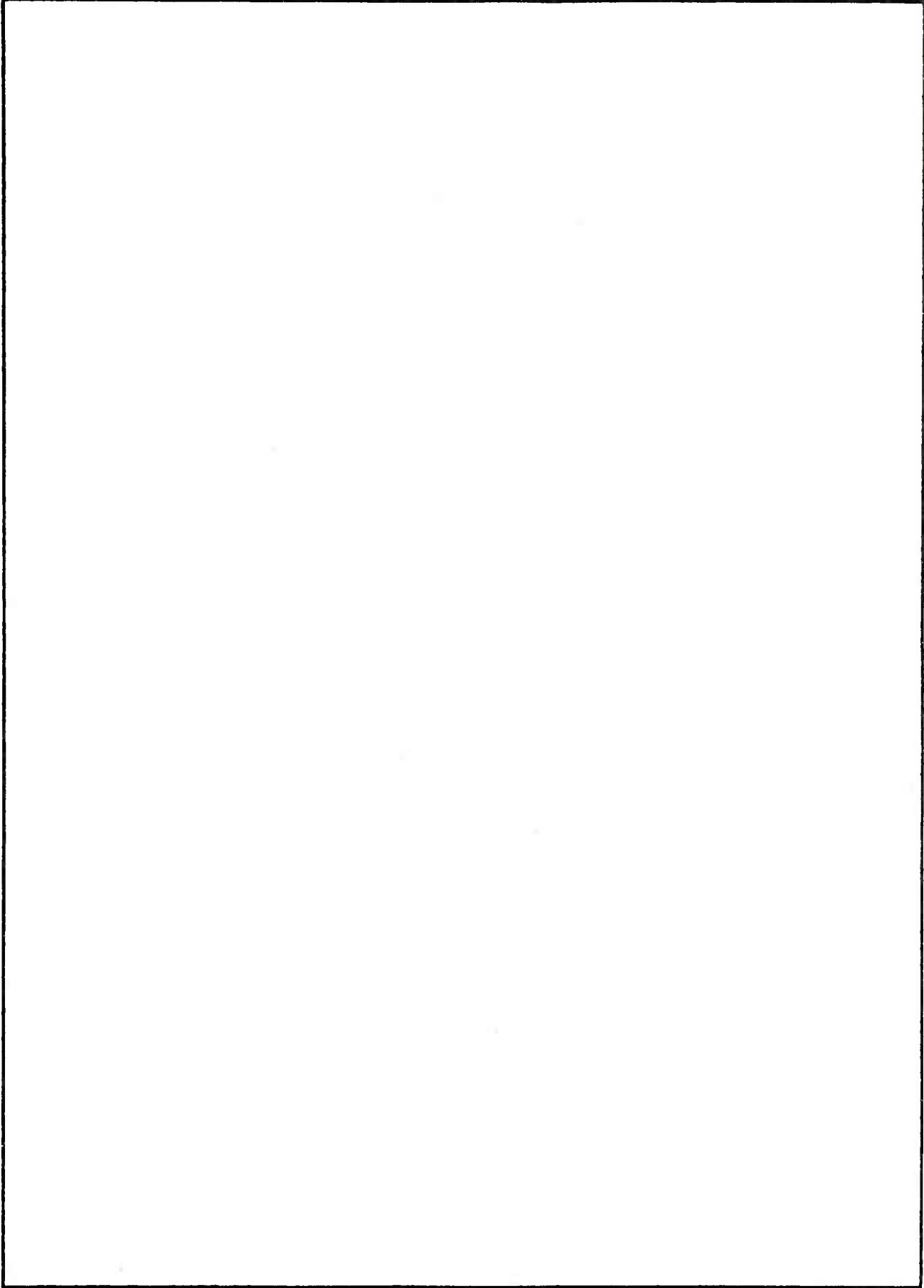
The views, opinions, and/or findings contained in this report are those of the author(s) and should not be construed as an official Department of the Army position, policy, or decision, unless so designated by other documentation.

The citation in this report of the names of commercial firms or commercially available products or services does not constitute official endorsement by or approval of the U.S. Government.

Destroy this report when no longer needed. Do not return to the originator.

REPORT DOCUMENTATION PAGE		READ INSTRUCTIONS BEFORE COMPLETING FORM
1. REPORT NUMBER Technical Report ARLCD-TR-84030	2. GOVT ACCESSION NO.	3. RECIPIENT'S CATALOG NUMBER
4. TITLE (and Subtitle) METAL ARMATURES FOR RAILGUNS		5. TYPE OF REPORT & PERIOD COVERED Final 1982 - 1984
7. AUTHOR(s) Gerald L. Ferrentino Willem J. Kolkert		6. PERFORMING ORG. REPORT NUMBER
9. PERFORMING ORGANIZATION NAME AND ADDRESS ARDC, LCWSL Applied Sciences Div (SMCAR-LCA-G) Dover, NJ 07801-5001		8. CONTRACT OR GRANT NUMBER(s)
11. CONTROLLING OFFICE NAME AND ADDRESS ARDC, TSD STINFO Div (SMCAR-TSS) Dover, NJ 07801-5001		10. PROGRAM ELEMENT, PROJECT, TASK AREA & WORK UNIT NUMBERS
14. MONITORING AGENCY NAME & ADDRESS (if different from Controlling Office)		12. REPORT DATE March 1985
		13. NUMBER OF PAGES
		15. SECURITY CLASS. (of this report) Unclassified
		15a. DECLASSIFICATION/DOWNGRADING SCHEDULE
16. DISTRIBUTION STATEMENT (of this Report) Approved for public release; distribution unlimited.		
17. DISTRIBUTION STATEMENT (of the abstract entered in Block 20, if different from Report)		
18. SUPPLEMENTARY NOTES Willem J. Kolkert has been on official leave from Prins Maurits Laboratorium TNO, The Netherlands, as a special projects officer with the U.S. Army ARDC, sponsored by the U.S. Army DARCOM Headquarters.		
19. KEY WORDS (Continue on reverse side if necessary and identify by block number)		
Armature	Frictional heating	Electromechanics
Railgun	Preload force	Finite-element analysis
Sabot	Armature fiber	Heat transport
Rail-armature interface	X-ray shadowgraph	
Penetrator	Range	
20. ABSTRACT (Continue on reverse side if necessary and identify by block number) Proper design of a metal armature for a railgun projectile is vital to obtain optimal performance and to reduce rail wear. Previous armature designs did not include the contribution of friction to the heat of the rail-armature interface. A simplified model of the electromechanical heating of the armature was developed and used to redesign an armature for the EMACK railgun at the Armament Research and Development Center. A new integrated armature-sabot package was constructed and test-fired.		

SECURITY CLASSIFICATION OF THIS PAGE(When Data Entered)



SECURITY CLASSIFICATION OF THIS PAGE(When Data Entered)

#### ACKNOWLEDGMENTS

The authors gratefully acknowledge H. Moore, W. Williams, J. Pappas, C. Dunham, B. Nagle, D. Witkowski, J. Daus, A. Zielinski, G. Zsidisin, K. Jamison, D. Scherbarth, T. Valko, and S. Scuro for contributions to the construction of the armature test vehicle and performing the EMACK experiments. We would also like to thank H. D. Fair, P. J. Kemmey, and T. F. Gora for their continued support and interest.

## CONTENTS

	Page
Introduction	1
Action Integral Considerations	2
Frictional Effects on Armature Mass	2
Results	5
Conclusions	5
References	7
Appendix - Derivation of Inner Equations in Motion and Armature Mass Equations	21
List of Symbols	27
Distribution List	28

## FIGURES

	Page
1 Original Westinghouse lexan cube projectile for EMACK railgun testbed	9
2 EMACK cube projectiles: new (right) and fired (left)	10
3 EMACK cube projectiles with respective accelerator rails: new (right) and fired (left); projectiles are at starting positions	11
4 Closeup of EMACK accelerator rails; left rail accelerated a lexan cube projectile from left to right, and right rail is new	12
5 Mechanical model for the normal force	13
6 Redesigned EMACK projectile	14
7 Effect of varying frictional heating of armature interface upon its mass	15
8 Remains of redesigned EMACK projectile	16
9 Closeup of redesigned EMACK projectile rush surfaces	17
10 Flash x-ray photograph of redesigned EMACK projectile in flight	18
11 Comparison of new EMACK rail (bottom) with that used to accelerate redesigned projectile (top)	19
12 Closeup of new EMACK rail (bottom) and that used to accelerate redesigned projectile (top)	20

## INTRODUCTION

The simplest way of electromagnetically propelling a projectile is by means of a metallic armature placed between two parallel conducting rails. The Lorentz forces generated by the interaction of the magnetic fields and currents accelerate the round and attach the armature down the bore of the railgun. During this process, the temperature of the metallic armature is increasing by ohmic heating while the rail armature interface is also heated by friction. The degree of heating (or rise in material temperature) affects the mechanical integrity of the armature, especially its rail interfaces. If an armature interface fails, anomalous rail wear as well as degraded gun performance occurs.

A properly designed armature will maintain an interface voltage below the threshold of arcing. Optimal energy transfer to the launch package will occur with the lowest possible barrel wear. This report discusses the effect of frictional interfacial heating, wear, and mechanical confinement on the design of a metal armature for a large railgun accelerator system.

Before the installation of the EMACK launcher at ARDC, railgun experiments with both metal and plasma armatures were conducted at the Australian National University (ANU) (ref 1) and at the Westinghouse Research and Development Center (refs 2 through 4). The design of the metal armatures described in this report is based on the work performed at these facilities.

The early ANU armatures were stacks of metal chevron leaves. Failure and detachment of the rear leaf, observed in several shots was explained by the velocity and temporal skin effects. During the initial switching of current into the gun and at velocities approaching 1 km/s, the skin effect causes the majority of the current to flow in the rear leaf of the stack. This causes accelerated heating and wearing of the leaf. After the leaf loses contact with the rails, it arcs and detachment occurs.

During the design and construction of EMACK, the Westinghouse Corporation performed theoretical and experimental work on metal armatures. The theoretical work (ref 2) analyzes the mechanical and electrical behavior of several simple designs. Experimentation was performed on a 12.7-mm bore gun powered with a 36-kJ capacitor bank, a 5- $\mu$ H storage inductor, and peak currents of 100 kA (ref 3). Armature designs similar to the ANU types were tried without much success. Then an armature constructed from a bundle of welding cable fibers was fired. Early results supported feasibility of constructing a solid armature that would not cause severe rail wear or arc damage. However, this type of armature does not lend itself to the simple electromechanical analysis of the chevron leaf or staple leaf designs.

In order to evaluate the thermal limitations of metal armatures, a series of experiments were conducted with trailing leaf chevron armatures. A detailed analysis of the mechanical behavior similar to that in the EMACK Phase I report was performed (ref 2). The thermal and electrical limitations were investigated experimentally using the ELF-I system (ref 3). Results indicated that the predominant failure mechanism for metal armatures with a proper mechanical design and with velocities of about 300 m/s was frictional heating of the rail-armature interfaces.

During the commissioning tests of the EMACK system at the Westinghouse Research and Development Center, a simple metal fiber brush armature was designed, fabricated, and fired (ref 4). It consisted of two copper welding cables mounted by fixtures to a 2-inch plexiglass cube (fig. 1). A similar design with smaller diameter cable was then fired at the ARDC site. A soft catch of one of these launch packages was performed in the second shot (fig. 2). The armature from the recovered remnants shows damage from severe arcing and vaporization. The rails showed evidence of a copper-aluminum deposition along the first 1.5 m of rail length (figs 3 and 4). The predominant cause of armature failure was an abnormally high degree of frictional heating of the armature due to the absence of a well-defined mechanical structure to restrict the motion of the fiber ends.

### ACTION INTEGRAL CONSIDERATIONS

The fundamental consideration that has commonly been used to predict the integrity of a metal armature is the action integral. Simply stated, the action integral is the bulk ohmic heating of a conductor that relates the current flow through the metal to a rise in its bulk temperature. This quantity has been analytically evaluated for an inductively driven lossless railgun. By using the evaluated expression for the action integral and the action constant, a quartic equation was derived to estimate the armature mass. This equation relates the armature mass ( $M_A$ ) to the penetrator and sabot masses ( $M_L$ ), material properties, and gun circuit parameters.

The quartic equation

$$\left(\frac{M_L}{M_A}\right)^4 + \left(\frac{M_L}{M_A}\right)^3 - \left(\frac{M_L}{M_C}\right)^3 = 0 \quad (1)$$

with

$$M_C = \left[ \rho \omega \left( \frac{L' \ell}{(L_o + L' \ell) L_o} \right)^{1/4} \left( \frac{2L_o I_o}{L' g_1} \right)^{1/2} \right]^{4/3} \quad (2)$$

can be readily solved (ref 5). A program was written in BASIC for the IBM PC and the effect of penetrator and sabot masses was evaluated.

### FRICTIONAL EFFECTS ON ARMATURE MASS

The mechanical strength of a material is related to its temperature and to the applied stress. Consequently, mechanical wear processes are related to armature interface temperatures, contact pressure, and sliding velocity. Because thermal diffusion or conduction processes are slower than electrical diffusion,

frictional heating of the rail armature contact must be added to the ohmic heating to calculate interface temperature. These armatures are composed of metal fibers; therefore, electrical skin effects are neglected.

In the region of the railgun near the armature, it is assumed that the current in the conductors creates a uniform magnetic field along the surface of the armature. For the armature section shown in figure 5, the contact force normal ( $F_N$ ) to the rail surface is

$$F_N = \left[ \frac{\Delta L \sin \theta}{\omega} \right] \frac{L I^2}{2} + F_P \quad (3)$$

The fiber bundle is modeled as a cantilevered beam. During the acceleration period, the fiber-to-fiber frictional force is assumed to be substantially less than the shear strength of a solid conductor. This lets the fiber bundle rotate about its hinge point without curvature.

Electrical skin effects are not included in this analysis. The discharge current flows uniformly throughout the volume of interest [bounded by an area parallel to the rail surface, to a depth ( $\delta$ ) of 0.90 mm]. The material of interest is copper with an action constant ( $g_1$ ) of 87.7 GJ/m at 1085°C. The rail armature interface is assumed to be molten copper with a coefficient of sliding friction ( $\mu$ ) of 0.05. The entire depth of 0.90 mm of copper is assumed to wear uniformly during the motion. From the mass point of view, the fiber bundle is assumed to be a block of solid copper.

A preload force ( $F_p$ ) of 2778 N, which linearly decays through acceleration, was calculated on the basis of a required minimum of 1 g/A contact force at the interface. Friction heat was calculated on the basis of the lossless railgun equations. This heat, shared equally by the rails and the armature, is uniformly deposited throughout the armature volume near the rail interface.

An armature and sabot body were designed with the considerations of the required preload forces, fiber length and compliance, shape of the armature conductors, confinement of the armature structure, and a sustained molten copper interface. This test vehicle (fig. 6) was then fabricated for the purpose of testing with the EMACK system.

The derivation of the self-consistent quartic equation is slightly different from that of the previous one in that a solution is found for the cross-sectional area of the armature rather than for armature mass. A term that represents the energy loss due to friction is added to the ohmic heating of the volume. This expression is equated to the heat content of the volume. From this equation the quartic equation for the cross-sectional area ( $A$ ) of the armature is derived to be

$$A^4 + 2a_1 A^3 + a_1^2 A^2 - a_2^2 \rho \omega A - a_2^2 M_L = 0 \quad (4)$$

where the coefficients are

$$a_1 = \left( \frac{\langle \sigma \rangle \mu}{2\delta g_1} \right) \left( \frac{\Delta L \sin \theta L I_o^2 L' \ell}{2\omega (L_o + L' \ell)} + F_{p\ell} \right) \quad (5)$$

and

$$a_2 = \left( \frac{2L' \ell I_o}{L' g'} \right) \left( \frac{L' \ell}{L_o (L_o + L' \ell)} \right)^{1/2} \quad (6)$$

Another program was written to analyze the effects of frictional heating upon the armature mass by use of this quartic equation. This program uses a more general solution to the quartic and includes more data concerning the metal armature. A sensitivity constant (H) was incorporated into the frictional terms (eq 5) so that a parametric relation between friction, wear, and armature mass could be obtained (fig. 7). The relationship of the armature mass to the sensitivity factor is almost linear over small regions (fig. 7).

ARDC and the Westinghouse R and D Center jointly constructed an armature test vehicle from an ARDC design. Minor modification will allow specialized projectiles to be launched for the investigation of hypervelocity terminal ballistics. The Westinghouse Corporation fabricated the fiber brush armature structures. The sabot body, made of G-11, did not break up during acceleration. An attempt was made to catch the vehicle softly in cotton rags. Due to the high velocity (about 1500 m/s as deduced from the dI/dt measurement at the storage inductor) and the heavy mass (about 500 g), the package was destroyed upon impact with the rear wall of the catch tank.

A slight modification was made to the sabot and a second shot at 560 m/s (measured from dB/dt probes along the barrel) was made with a launch package mass of 550 g. Even with the lower velocity and fortified soft catch structure in the catch tank, the package impacted the rear wall of the catch tank (fig. 8). The brush remnants, which were intact enough to examine, showed no evidence of armature arcing (fig. 9). In-flight x-ray shadowgraphs of the vehicle, which were also obtained at two different positions in the range tank, indicate that the package was intact and the brushes showed minimal wear (fig. 10). A post-shot examination of the barrel also showed that no arcing occurred during launch except for a 6- to 7-inch long section at the gun muzzle.

The most interesting result of both experiments is that the type of severe rail erosion or wear at the breech region that has been typically reported in experiments by others did not occur (figs. 11 and 12). This means that, with proper electromagnetic design of the fiber brushes and proper selection of the rail material, minimal barrel erosion can be obtained for electromagnetic gun applications incorporating metal armature propulsion.

## RESULTS

The assumed model for the rail-armature interface was useful for choosing armature masses that performed satisfactorily. However, the model does not yield insight on the detailed mechanics and physical behavior of metal brushes. Other experiments are required to evaluate armature designs that allow greater brush wear, or that employ finer fibers in the brushes. Such armature designs may be required for useful sliding contacts at velocities over 1.5 km/s.

Further theoretical analyses are required to support the EMACK solid armature experiments. An integrated electromechanical finite-element analysis of the behavior of sliding brushes would be especially valuable. Another useful model should be developed to include the heat transport at the rail-armature interface. This analysis would enable armature designs to be corrected for fiber wear and thermal expansion. With this type of modeling and experimental verification, an evaluation of the impact of solid metal armatures in military applications can be made.

## CONCLUSIONS

The model and experiments demonstrate the importance of including frictional heating effects at the rail-armature interface in the design of a railgun system and in the prediction of its performance. The test vehicles which were designed for the EMACK launcher led to a more efficient transfer of energy to the launch package with minimal rail wear by designing for frictional heating and fiber wear. However, further experiments and modeling are required for a more detailed understanding.

## REFERENCES

1. R. A. Marshall, "Moving Contacts in Macro-Particle Accelerators," proceedings of the Australian, U.S. seminar on Energy Storage, Compression and Switching, November 15 - 20, 1977, High Power, High Energy Pulse Production and Application, E. Inall, ed., ANU Press, Canberra, Australia, pp 216-230, 1978.
2. I. R. McNab, "DC Electromagnetic Launcher Development: Phase I," Contractor Report ARLCD-CR-80009, ARRADCOM, Dover, NJ, May 1980.
3. D. P. Ross, G. L. Ferrentino, and F. J. Young, "Experimental Determination of the Contact Friction for an Electromagnetically Accelerated Armature," Wear, 78 (1982), pp 189.
4. D. W. Deis, D. W. Scherbarth, and G. L. Ferrentino, "EMACK Electromagnetic Launcher Commissioning," Second Symposium on Electromagnetic Launch Technology, Boston, Massachusetts, October 10 - 13, 1983.
5. M. Abramowitz and I. A. Stegun editors, Handbook of Mathematical Tables, Dover Publications, Inc., New York, 1965.



Figure 1. Original Westinghouse lexan cube projectile for EMACK railgun tested



Figure 2. EMACK cube projectiles: new (right) and fired (left)

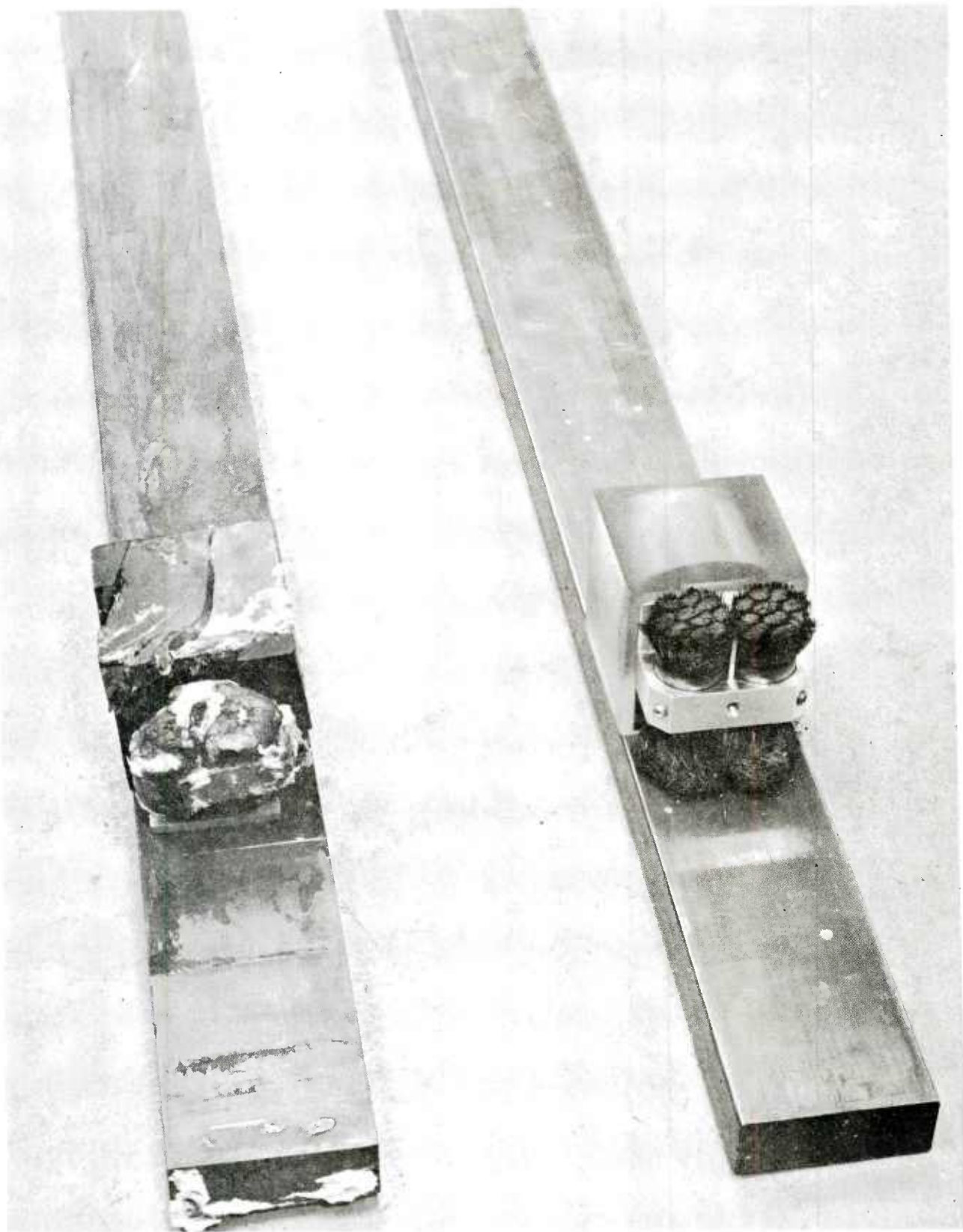


Figure 3. EMACK cube projectiles with respective accelerator rails: new (right) and fired (left); projectiles are at starting positions

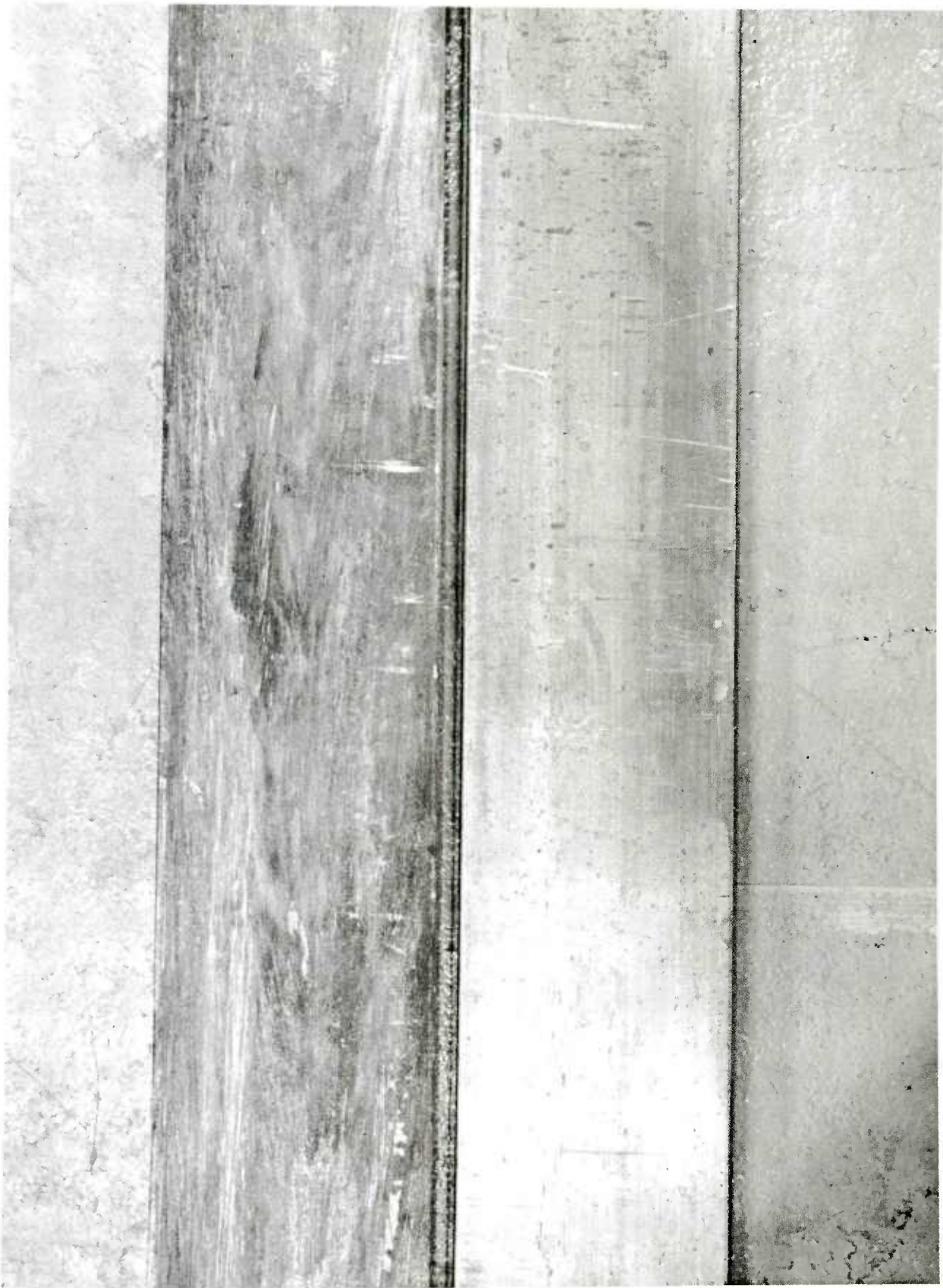


Figure 4. Closeup of EMACK accelerator rails; left rail accelerated a lexan cube projectile from left to right, and right rail is new

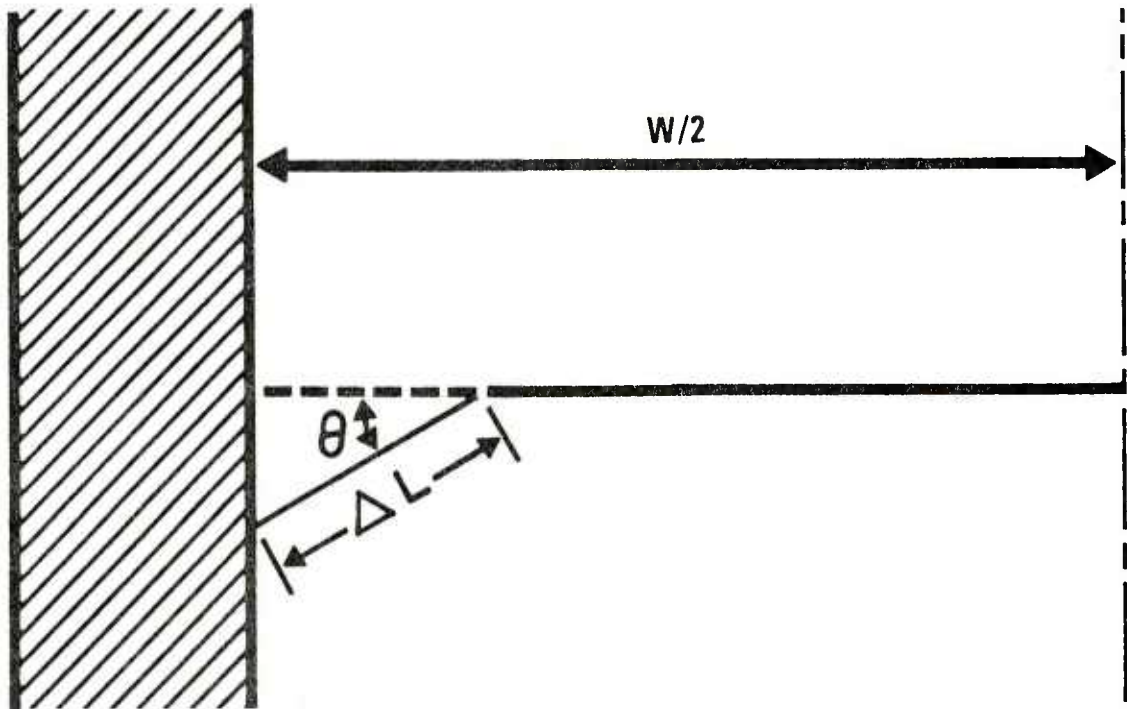


Figure 5. Mechanical model for the normal force

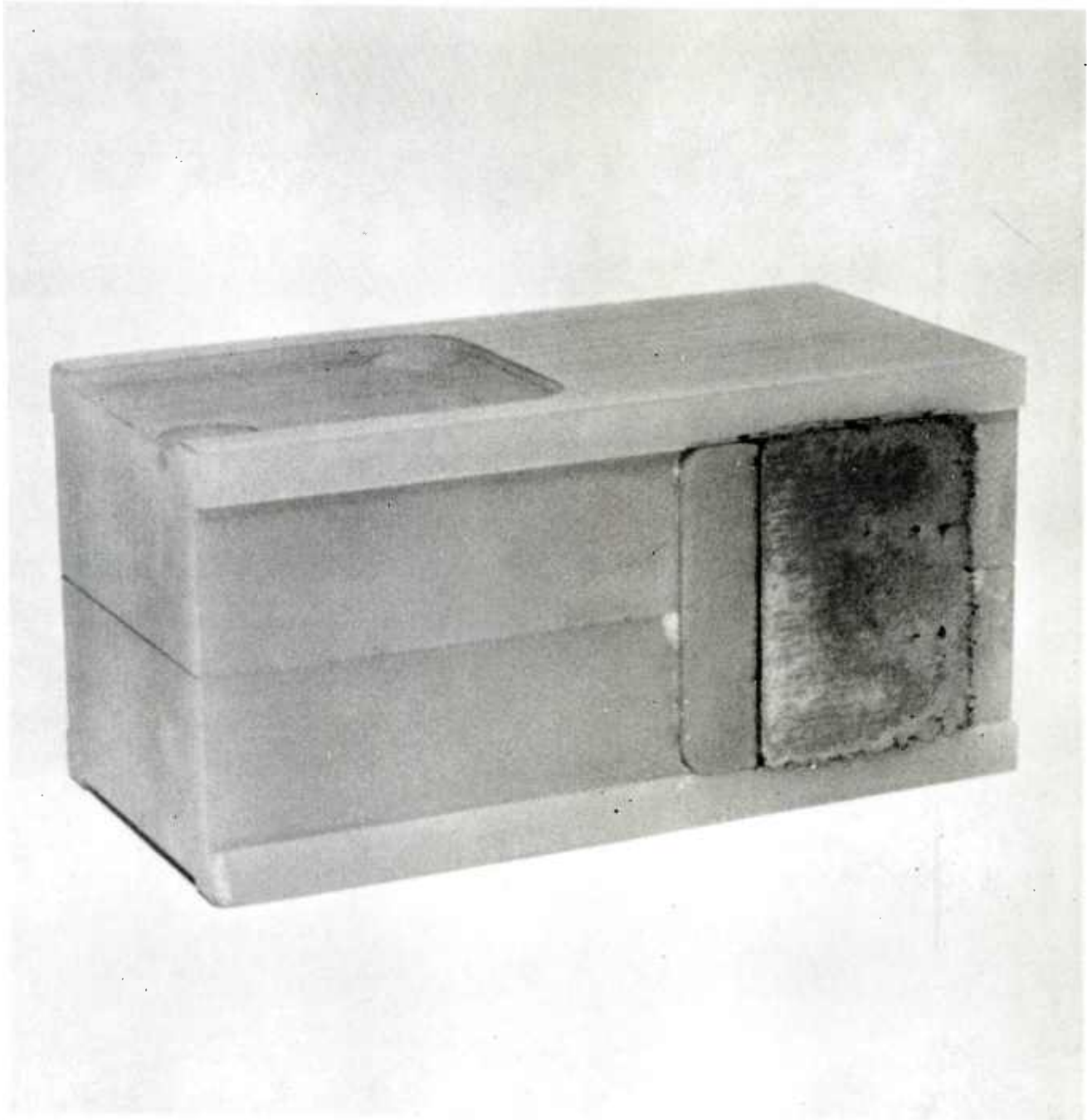


Figure 6. Redesigned EMACK projectile

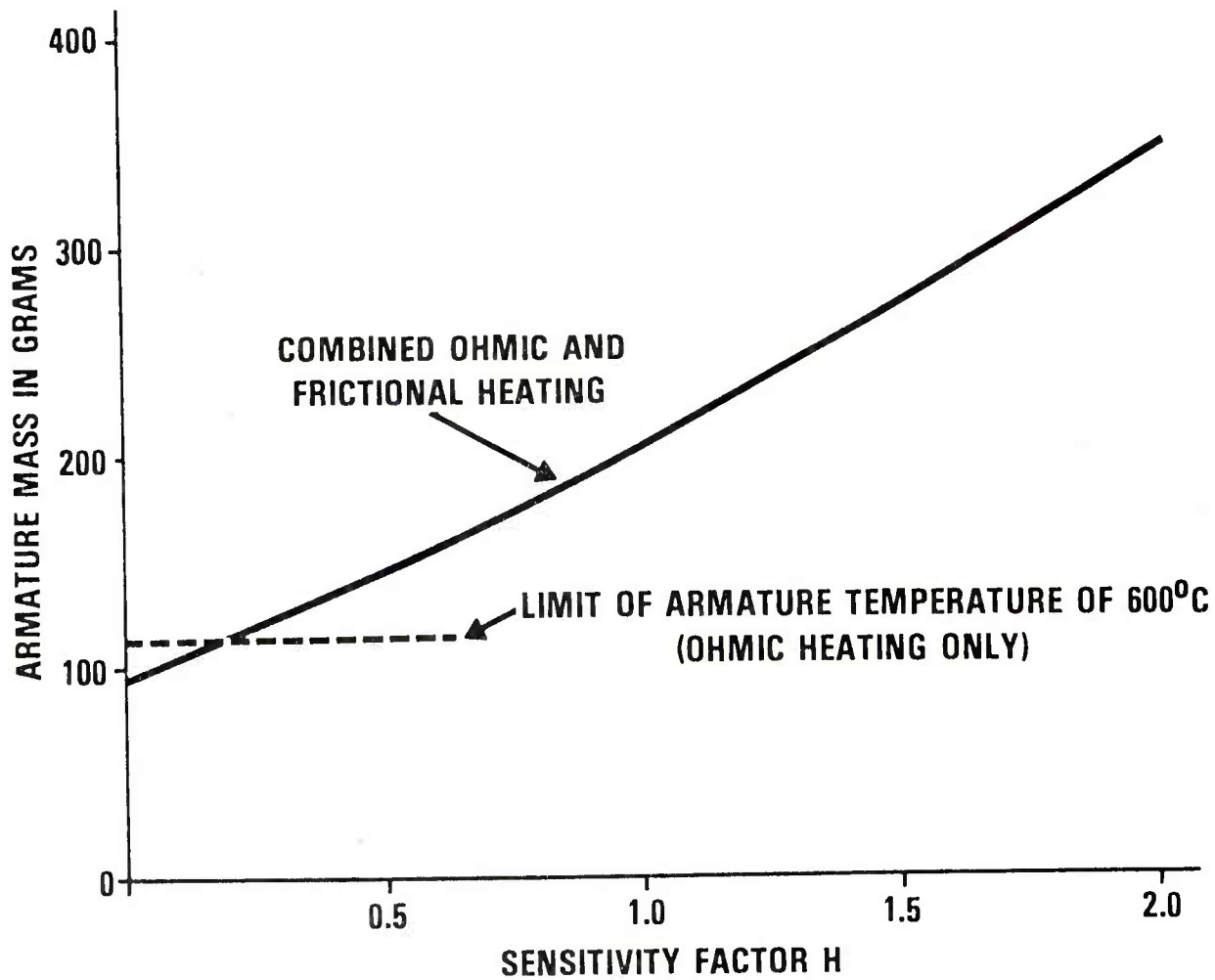


Figure 7. Effect of varying frictional heating of armature interface upon its mass

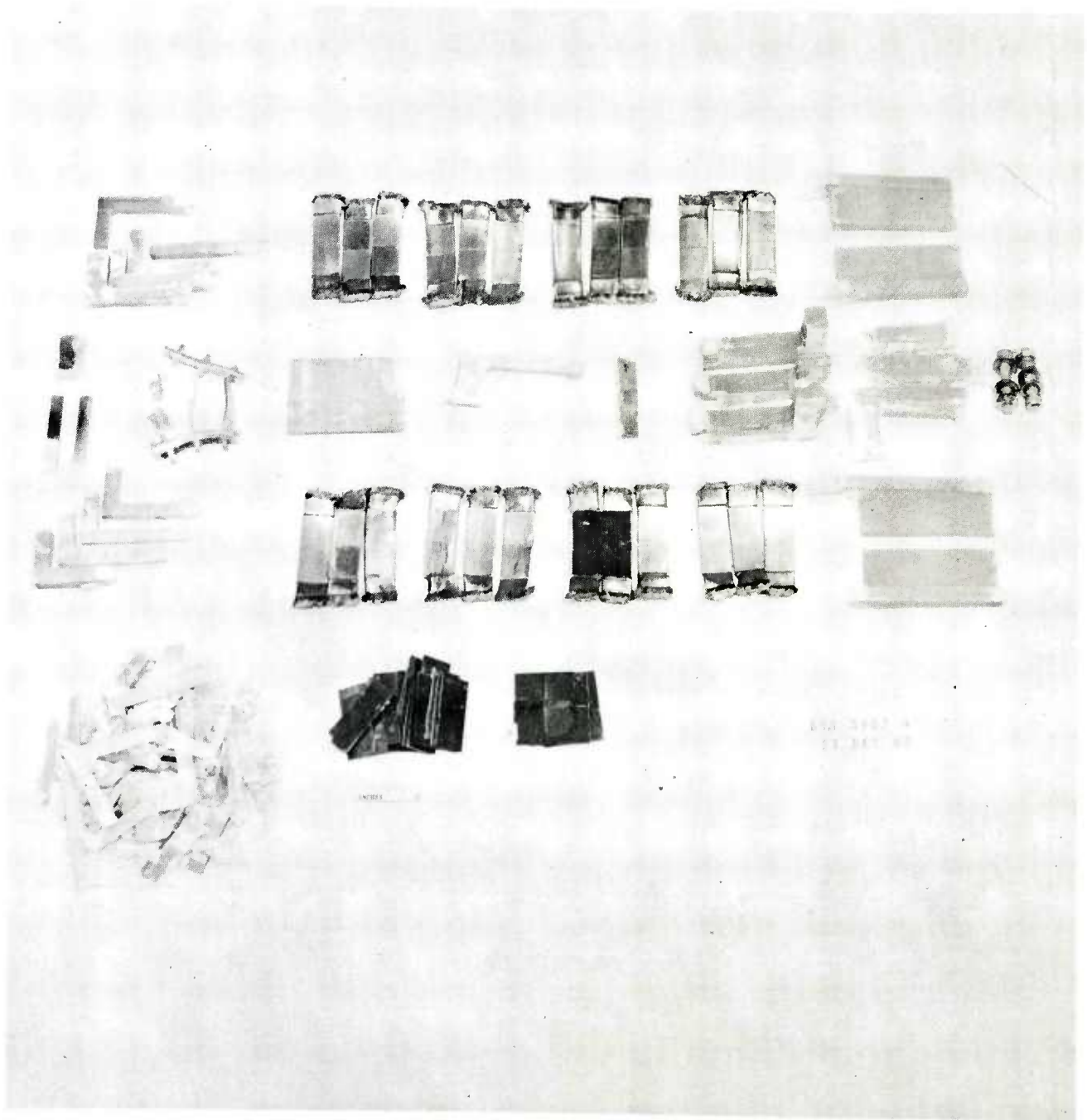


Figure 8. Remains of redesigned EMACK projectile



Figure 9. Closeup of redesigned EMACK projectile brush surfaces

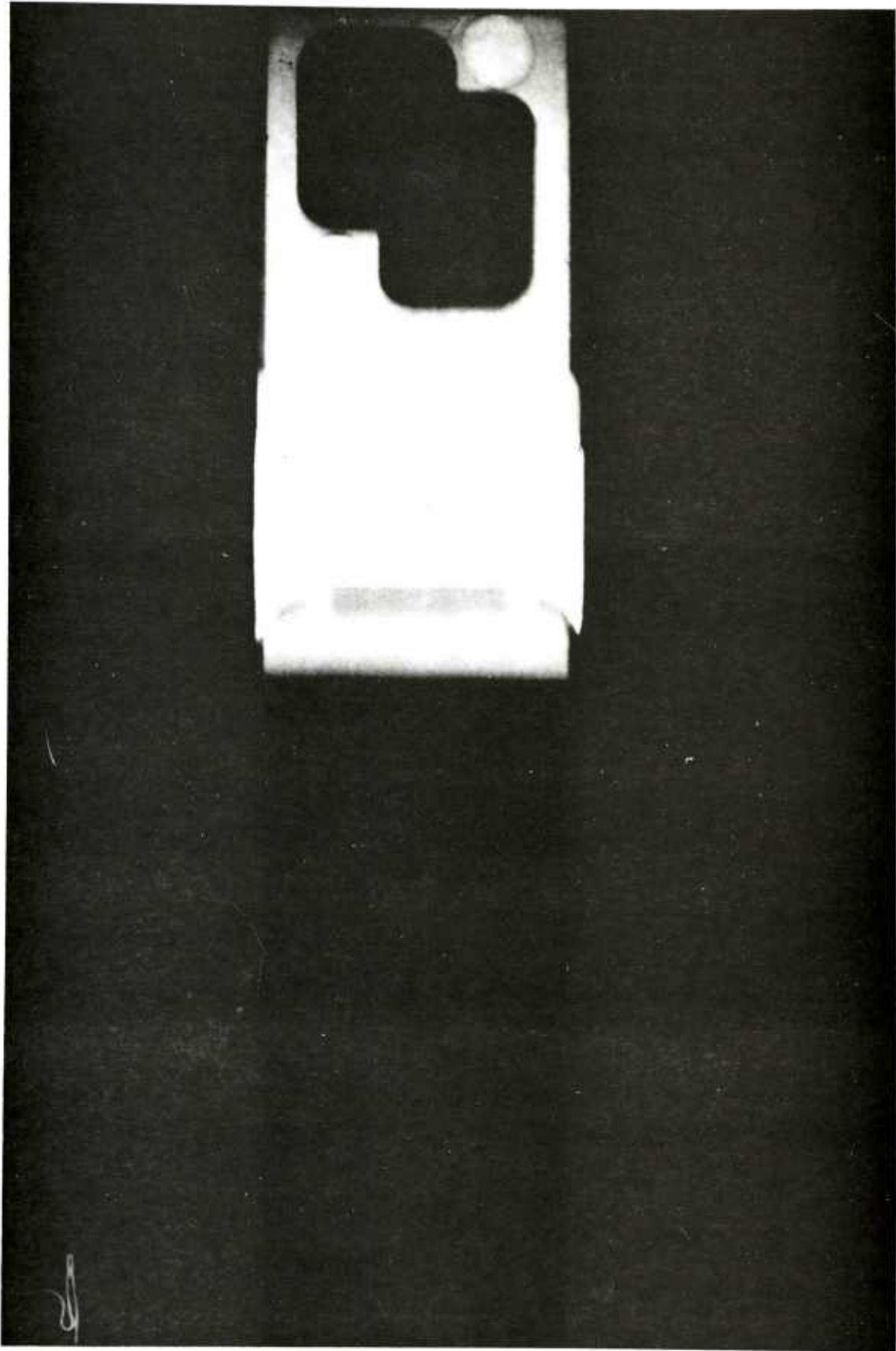


Figure 10. Flash x-ray photograph of redesigned EMACK projectile in flight

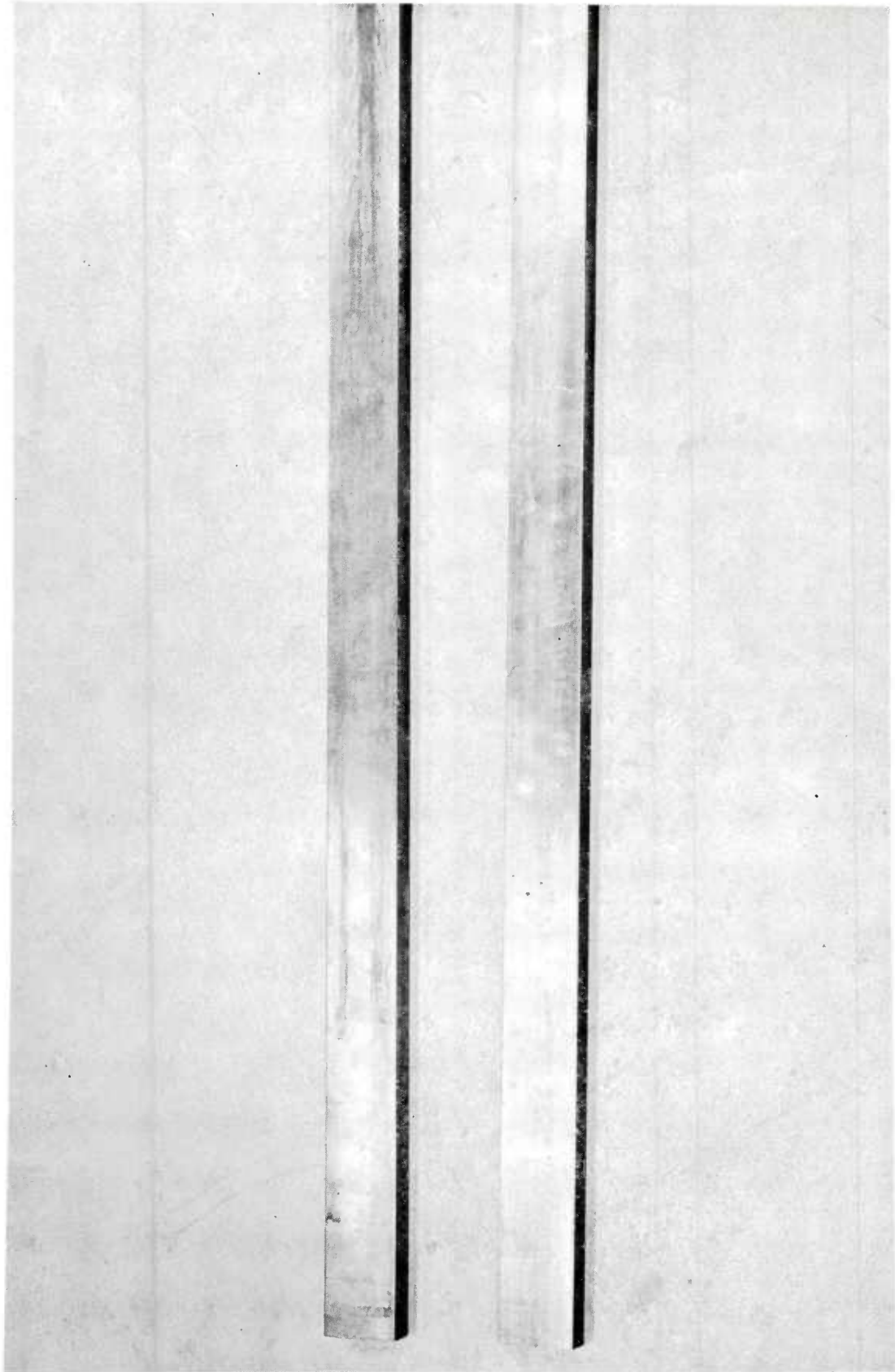


Figure 11. Comparison of new EMACK rail (bottom) with that used to accelerate redesigned projectile (top)

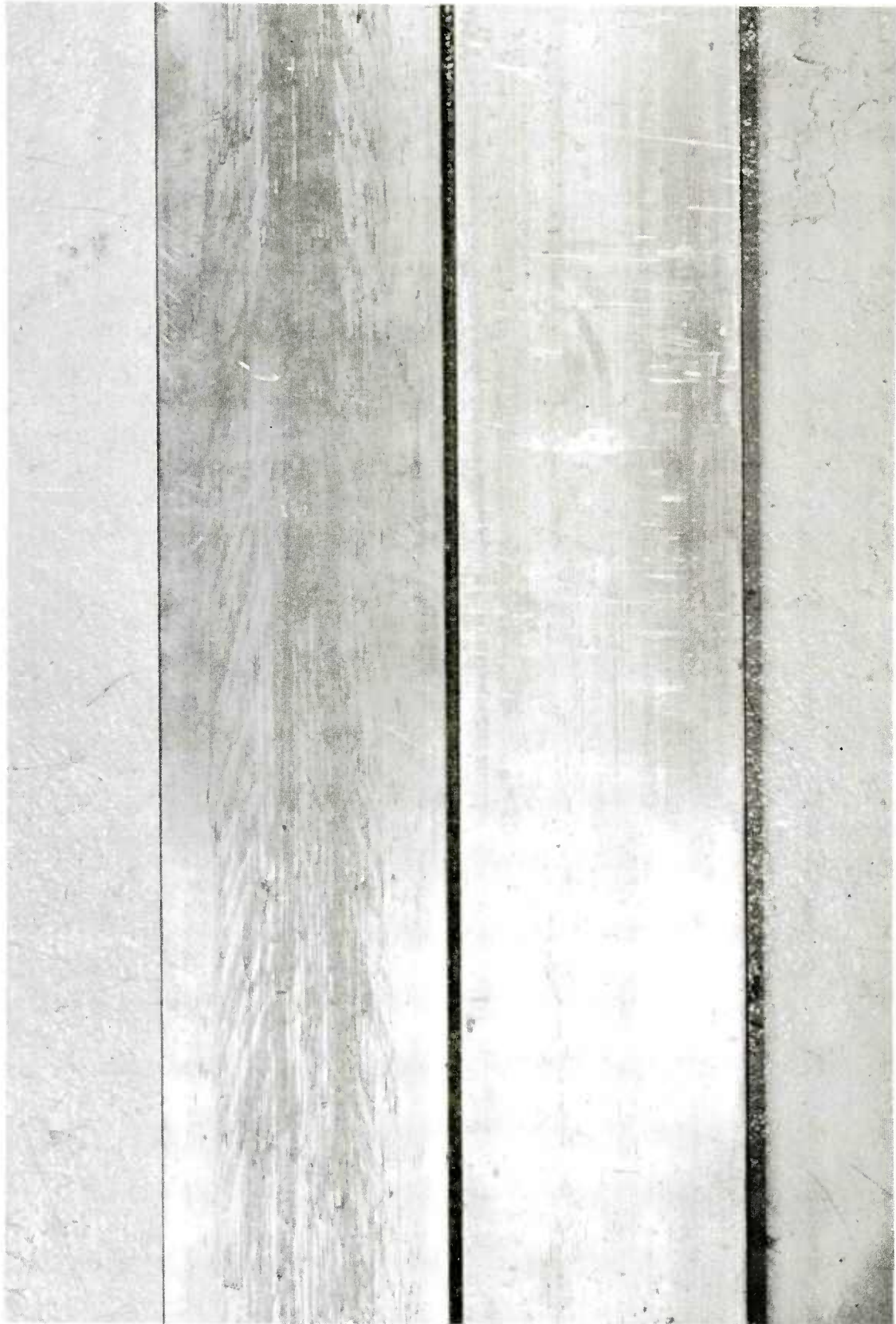


Figure 12. Closeup of new EMACK rail (bottom) and that used to accelerate redesigned projectile (top)

APPENDIX

DERIVATION OF INNER EQUATIONS IN MOTION AND ARMATURE MASS EQUATIONS

## Interior Ballistics of a Lossless Railgun

The following derivation describes the fundamental interior equations of motion of a projectile in a railgun. The launcher circuit is a lossless inductor coupled to a lossless railgun and metal armature.

### Interior Force Law

The accelerating force on the projectile is given by

$$(M_A + M_L) d^2x/dt^2 = \frac{1}{2} L' I^2 \quad (A-1)$$

This relationship was discovered by Ampere.\*

### Conservation of Flux

Since the gun circuit is lossless, the flux linkages are constant during the acceleration of the projectile. The flux linkages lost by the storage inductor are equal to the increase of flux linkages in the railgun barrel. The kinetic energy gained by the projectile is equal to the energy lost by the coupled inductive circuit. With these considerations, the circuit current as a function of projectile displacement,

$$I = I_0 [L_0 / (L_0 + L'x)] \quad (A-2)$$

### Interior Equations of Motion

Equation A-1 with the aid of A-2 can be successively integrated to determine projectile velocity as a function of displacement,

$$v = \left( \frac{L_0 I_0^2 L'x}{(M_A + M_L) (L_0 + L'x)} \right)^{1/2} \quad (A-3)$$

---

\* Volume II of Maxwell's Treatise on Electricity and Magnetism.

and time as a function of projectile displacement

$$t = \left( \frac{M_A + M_L}{L' I_o^2} \right)^{1/2} \left[ \left( \frac{L'x}{L_o} \right)^2 + \frac{L'x}{L_o} \right]^{1/2} + \ell n \left( \sqrt{\frac{L'x}{L_o}} + \sqrt{\frac{L'x}{L_o}} + 1 \right) \quad (A-4)$$

## Thermal Equations

### Ohmic Dissipation

The balance between the ohmic dissipation and the Joule heating of a metallic conductor with a uniform current cross section and with a uniform density is

$$(I/A)^2 / \sigma = \rho c \frac{dT}{dt} \quad (A-5)$$

With a simple algebraic manipulation, this equation can be integrated to give

$$\int I^2 dt = g l A^2 \quad (A-6)$$

If there is not heat loss from the conductor, the mechanical and electrical properties of a metal are uniquely determined by the action integral ( $\int I^2 dt$ ).

### Frictional Dissipation

The energy lost to friction is calculated by

$$\mu_o \int \ell F_N dx = \frac{\mu}{2} \left[ \frac{\ell L_o I_o^2 L'x}{\omega 2 (L_o + L'x)} + \frac{F_p \ell}{2} \right] \quad (A-7)$$

The model described in this report assumes equal heating of the rails and armature interfaces.

## Armature Mass Equations

### Frictionless Case

The armature mass is determined by

$$M_A = \rho \omega \sqrt{\frac{\int I^2 dt}{g_1}} \quad (\text{A-8})$$

for the frictionless railgun. If the gun is also lossless, the action integral is

$$\int I^2 dt = \frac{2I_o}{L'} \sqrt{\frac{L_o L' x (M_A + M_L)}{L_o + L' x}} \quad (\text{A-9})$$

Substitution of A-9 into A-8 gives

$$\left(\frac{M_L}{M_A}\right)^4 + \left(\frac{M_L}{M_A}\right)^3 - \left(\frac{M_L}{M_C}\right)^3 = 0$$

### Case with Frictional Effects

The energy lost to friction can be added to the ohmic dissipation in the armature volume that will be worn away during the acceleration cycle. With the assumptions of fixed amount of wear and of average conductivity to weight the frictional contribution, the cross-sectional area of the metal armature is determined by

$$\int I^2 dt = g_1 A^2 - \frac{\mu \langle \sigma \rangle}{2\epsilon} A \int_0^L F_N dx \quad (\text{A-10})$$

Substitution of A-9 into A-10 and algebraic manipulation give

$$A^4 + 2a_1 A^3 + a_1^2 A^2 - a_2^2 \rho \omega A - a_2^2 M_L = 0$$

## LIST OF SYMBOLS

$M_A$	Armature Mass
$M_L$	Penetrator and sabot mass
$M_C$	Minimum armature mass ( $M_L = 0$ )
$\omega$	Rail separation
$\Delta L$	Length of chevron leaf
$\theta$	Cant angle of chevron leaf
$\rho$	Armature material density
$L_0$	Storage inductance of gun circuit
$I_0$	Initial current of gun circuit
$L'$	Inductance gradient of gun barrel
$C$	Specific heat of armature material
$g_1$	Action constant of armature material
$l$	Length of barrel
$I$	Gun circuit current
$F_N$	Normal force at armature rail interface
$F_p$	Armature preload force
$A$	Armature cross-sectional area
$\langle\sigma\rangle$	Average armature electrical conductivity
$\delta$	Depth of armature wear
$\mu$	Coefficient of sliding friction
$H$	Sensitivity constant to examine effect of friction and to evaluate assumptions of the model
$t$	Time
$x$	Projectile displacement in the barrel
$T$	Temperature

DISTRIBUTION LIST

Commander  
Armament Research and Development Center  
U.S. Army Armament, Munitions  
and Chemical Command  
ATTN: SMCAR-LCA-G (18)  
SMCAR-TSS (5)  
SMCAR-SF  
Dover, NJ 07801-5001

Commander  
U.S. Army Armament, Munitions  
and Chemical Command  
ATTN: AMSMC-GCL(D)  
AMSMC-QAR-R(D)  
Dover, NJ 07801-5001

Administrator  
Defense Technical Information Center  
ATTN: Accessions Division (12)  
Cameron Station  
Alexandria, VA 22314

Director  
U.S. Army Materiel Systems  
Analysis Activity  
ATTN: DRXSY-MP  
Aberdeen Proving Ground, MD 21005-5066

Commander  
Chemical Research and Development Center  
U.S. Army Armament, Munitions  
and Chemical Command  
ATTN: SMCCR-SPS-IL  
Aberdeen Proving Ground, MD 21010-5423

Commander  
Chemical Research and Development Center  
U.S. Army Armament, Munitions  
and Chemical Command  
ATTN: SMCCR-RSP-A  
Aberdeen Proving Ground, MD 21010-5423

Director  
Ballistic Research Laboratory  
ATTN: AMXBR-OD-ST  
Aberdeen Proving Ground, MD 21005-5066

Chief  
Benet Weapons Laboratory, LCWSL  
Armament Research and Development Center  
U.S. Army Armament, Munitions  
and Chemical Command  
ATTN: SMCAR-LCB-TL  
Watervliet, NY 12189-5000

Commander  
U.S. Army Armament, Munitions  
and Chemical Command  
ATTN: AMSMC-LEP-L  
Rock Island, IL 61299-6000

Director  
U.S. Army TADOC Systems  
Analysis Activity  
ATTN: ATAA-SL  
White Sands Missile Range, NM 88002

Director  
Defense Advanced Research  
Projects Agency  
ATTN: DARPA-TTO, Dr. H. D. Fair, Jr.  
1400 Wilson Boulevard  
Arlington, VA 22317

Commander  
Ballistic Missile Defense System Command  
ATTN: BMD/ATC-M, Darrell Harmon  
P.O. Box 1500  
Huntsville, AL 35807

Center for Electromechanics  
ATTN: W. Weldon  
Taylor Hall 227  
University of Texas at Austin  
Austin, TX 78712

Commander  
HQ, AFSC/DLWA  
ATTN: CPT R. Reynolds  
Andrews Air Force Base, MD 20334

Commander  
Naval Sea Systems Command  
ATTN: LCDR, Joseph R. Costa  
Washington, DC 20362

Commander  
Air Force Armament Technology Laboratory  
ATTN: DLDG, Timothy Aden  
Eglin Air Force Base, FL 32542

Electromagnetic Launch Research, Inc.  
ATTN: Dr. Henry Kolm  
Dr. Peter P. Mongeau  
625 Putnam Avenue  
Cambridge, MA 92139

Dr. Ian R. McNab  
Westinghouse Electric Company  
Manager, EML Engineering  
Marine Division, MS ED-5  
401 E. Hendy Avenue  
P.O. Box 499  
Sunnyvale, CA 94088

Dr. James R. Powell, Jr.  
Head, Fusion Technology Group  
Brookhaven National Laboratory  
Building 820M  
Upton, NY 11973